

THE EMPIRICAL IMPACT OF REDUCING SYMMETRIES ON THE PERFORMANCE OF DEEP ENSEMBLES AND MOE

Andrei Chernov
Independent Researcher
chernov.andrey.998@gmail.com

Oleg Novitskij
HSE University
oanovitskii@edu.hse.ru

ABSTRACT

Recent studies have shown that reducing symmetries in neural networks enhances linear mode connectivity between networks without requiring parameter space alignment, leading to improved performance in linearly interpolated neural networks. However, in practical applications, neural network interpolation is rarely used; instead, ensembles of networks are more common. In this paper, we empirically investigate the impact of reducing symmetries on the performance of deep ensembles and Mixture of Experts (MoE) across five datasets. Additionally, to explore deeper linear mode connectivity, we introduce the Mixture of Interpolated Experts (MoIE). Our results show that deep ensembles built on asymmetric neural networks achieve significantly better performance as ensemble size increases compared to their symmetric counterparts. In contrast, our experiments do not provide conclusive evidence on whether reducing symmetries affects both MoE and MoIE architectures. The code is available on GitHub¹.

1 INTRODUCTION

In the last decade, neural networks have proven to be one of the most important algorithms in the field of machine learning. Despite their undeniable empirical success, many fundamental questions remain unanswered. One such question concerns parameter space symmetries: for any given set of neural network parameters, there exist numerous ‘twins’ that produce exactly the same output for every input while having different parameter values.

There are multiple sources of symmetry in neural network architectures. One prominent example is permutation symmetry in fully connected layers. Consider a standard multi-layer perceptron (MLP). If we swap two neurons in a hidden layer along with their incoming and outgoing weights, the network will produce the exact same output. As a result, any hidden layer of size n has $n!$ different sets of parameters that yield identical outputs. Activation functions such as ReLU Nair & Hinton (2010) can also produce symmetries Wiese et al. (2023).

The effects of parameter symmetries have been studied in various areas, including neuron interpretability Godfrey et al. (2022), optimization Neyshabur et al. (2015), and Bayesian deep learning Kurle et al. (2022). In this work, we primarily focus on the impact of symmetries on model accuracy. It has been shown in Lim et al. (2024) that eliminating redundant parameters in neural networks improves linear mode connectivity, thereby enhancing the performance of networks whose parameters are obtained by interpolating between two trained models. In this study, we present the Mixture of Interpolated Experts model (see Section 4.3 for details) and investigate how parameter symmetries influence its performance.

¹https://github.com/krds00/asym_ensembles/

However, the practical application of interpolated neural networks remains controversial, as such architectures usually do not provide a performance boost. The most common approach to leveraging multiple neural networks is through ensembles, where outputs from several models are aggregated to form a final prediction—examples include Deep Ensembles Lakshminarayanan et al. (2017) and Mixture of Experts (MoE) Fedus et al. (2022). In this paper, we empirically investigate how reducing symmetry impacts the performance of Deep Ensembles and MoE on 5 datasets.

2 RELATED WORK

2.1 W-ASYMMETRIC MLP

Various methods for breaking parameter symmetries in neural networks have been studied, including approaches to removing permutation symmetries Pourzanjani et al. (2017); Pittorino et al. (2022), scaling symmetries Badrinarayanan et al. (2015), and sign symmetries Wiese et al. (2023). However, in most of these approaches, the neural network architectures or training processes deviate from standard practices, making them difficult to apply in practice. In this work, we fully adopt the approach from Lim et al. (2024) to break symmetries in neural networks. This method randomly freezes a portion of the neural network’s weights before training, keeping them unchanged throughout training (see Section 4.1 for details). Notably, it does not require any special modifications to the training process. Authors of Lim et al. (2024) showed that breaking symmetries improves linear mode connectivity between two independently trained neural networks. In this paper, we investigate the empirical impact of reducing symmetries on the performance of Deep Ensembles and Mixture of Experts.

2.2 NEURAL NETWORK ENSEMBLES

In this study, we employ two different approaches for ensembling neural networks. The first approach, known as Deep Ensembles Lakshminarayanan et al. (2017), trains k neural networks independently and averages their outputs to obtain the final prediction.

The second approach is the Mixture of Experts (MoE) Yuksel et al. (2012), which consists of two main components: experts and a gating network. Each expert generates an output, but unlike Deep Ensembles, the final prediction is obtained through a weighted average of the experts’ outputs. The weights for each expert are dynamically predicted by the gating network rather than being fixed. Recently, MoE architectures utilizing MLP models as experts have gained popularity Fedus et al. (2022) especially in NLP Du et al. (2022) and CV domains Puigcerver et al. (2023); Riquelme et al. (2021). In this work, we adapt MoE architectures for tabular data from Chernov (2025). We cover it in detail in Section 4.2.

3 DATASETS

For our work, we selected five datasets to cover different problems:

- **Regression:** California Housing Prices dataset Pace & Barry (1997).
- **Binary classification:** Churn Modeling² and Adult Income Kohavi et al. (1996).
- **Multi-class classification:** MNIST Deng (2012) and Otto Group Product³.

Appendix A.1 summarizes the key attributes of these datasets. To ensure consistency, we applied a standardized preprocessing pipeline. Each dataset was split into training, validation, and testing sets with an overall

²<https://www.kaggle.com/shrutimechlearn/churn-modelling>

³<https://www.kaggle.com/c/otto-group-product-classification-challenge/data>

partitioning of 64% for training, 16% for validation, and 20% for testing. Real-valued features were scaled using a `StandardScaler`, and for classification tasks, the splits were stratified by the target variable. Additional preprocessing steps were applied to each dataset as follows:

- **Churn Modeling dataset:** Non-informative columns such as `RowNumber`, `CustomerId`, and `Surname` were removed.
- **Otto Group Product dataset:** The `id` column was dropped, and the target variable was encoded using a `LabelEncoder`.
- **Adult Income dataset:** The target variable was transformed by mapping $\leq \$50\text{K}$ to 0 and $> \$50\text{K}$ to 1. Categorical features were processed using a `OneHotEncoder`, with missing values imputed as `MissingValue`, while numerical missing values were filled with 0.
- **California Housing Prices dataset:** Since this dataset contains no missing values, its numerical features were simply scaled.
- **MNIST dataset:** Grayscale images were preprocessed by normalizing and centering pixel values.

4 MODELS

4.1 W-ASYMMETRIC MLP

In this paper, we fully adopt the implementation of W-Asymmetric MLP (WMLP) from Lim et al. (2024), where it was theoretically proven that this approach significantly reduces parameter symmetries. This is achieved by freezing a small portion of the weights, approximately $\mathcal{O}(n^{1/4})$ for details see Algorithm 1

It is important to emphasize that in ensemble networks utilizing different WMLP models, the frozen neurons—both in value and position—remain identical across all instances. For the hidden layers, we use the GeLU activation function from Hendrycks & Gimpel (2016) in both MLP and WMLP.

4.2 MIXTURE OF EXPERTS

In Chernov (2025), it was shown that MoE performs at least as well as a vanilla MLP on tabular data while requiring significantly fewer parameters. In this paper, we compare the performance of MoE with MLP as experts against MoE with WMLP experts.

From Chernov (2025), we utilize both the vanilla MoE, where logistic regression is used as a gating neural network, and the Gumbel Gating MoE (GG MoE), which employs the Gumbel-softmax function instead of the standard Softmax activation for logistic regression. Following the original paper, we use 10 samples from the Gumbel-softmax distribution during inference.

4.3 MIXTURE OF INTERPOLATED EXPERTS

Since Lim et al. (2024) demonstrated that reducing symmetries improves the performance of linearly interpolated neural networks, we evaluate the performance of the Mixture of Interpolated Experts (MOIE). MOIE uses the same gating function as MoE but, instead of computing a weighted average of the final outputs, it linearly interpolates the weights of the experts to produce an output:

$$\hat{y} = \text{Expert architecture} \left(\sum_i^k \alpha_i(x) W_i(x) \right),$$

Algorithm 1 WMLP Weight and Bias Initialization with Masking

Require: Number of layers $L = 4$, hidden dimension $d \in \{64, 128, 256\}$, and mask seeding parameter `mask_num`.

1: **Define fixed weights per output unit:**

$$n_{\text{fix}}^{(1)} = 2, \quad n_{\text{fix}}^{(l)} = \begin{cases} 4, & \text{if } d = 256, \\ 3, & \text{otherwise} \end{cases} \quad \text{for } l > 1.$$

2: **for** $l = 1, \dots, L$ **do**

3: Let $W^{(l)} \in \mathbb{R}^{\text{out}_l \times \text{in}_l}$ be the weight matrix.

4: **for** $i = 1, \dots, \text{out}_l$ **do**

5: **Generate Mask:**

6: For each output unit, select a random subset of $n_{\text{fix}}^{(l)}$ input indices to be fixed. The fixed positions are determined using a seed based on l and the output unit index, ensuring reproducibility within an ensemble.

7: **for** $j = 1, \dots, \text{in}_l$ **do**

8: **if** j is in the fixed subset for unit i **then**

9: Set $W_{ij}^{(l)} \sim \mathcal{N}(0, 1)$. The random seed for fixed weights depends on the layer l and weight position. These weights are then frozen.

10: **else**

11: Initialize $W_{ij}^{(l)}$ using Kaiming Uniform Initialization with parameter $\sqrt{5}$. The random seed for non-frozen weights depends on the repetition number, the estimator index in the ensemble, l , and the weight's position.

12: **end if**

13: **end for**

14: **end for**

15: **Initialize Bias:**

16: Set $b^{(l)}$ uniformly in

$$\left[-\frac{1}{\sqrt{\text{in}_l}}, \frac{1}{\sqrt{\text{in}_l}} \right],$$

▷ The random seed for bias initialization depends on the repetition number, the estimator index, l , and the bias position.

17: **end for**

where \hat{y} is the final prediction, k is the number of experts, α is an output from a gating network, and W_i represents the model parameters of each expert. The expert architecture is selected from MLP, WMLP.

5 EXPERIMENTS

5.1 SETUP

In this section, we describe the details of the training and evaluation procedures applied to Deep Ensembles (Section 5.1.1), MoE and MoIE (Section 5.1.2).

5.1.1 DEEP ENSEMBLE

We trained models with a batch size of 256. For constructing Deep Ensembles, we trained 64 instances of both the MLP and WMLP models, each initialized with a different random seed to ensure variability in the free weights.

For WMLP, a fixed number of random weights per row, denoted as n_{fix} , was selected and frozen in each layer. These frozen weights were sampled from a $\mathcal{N}(0, I)$ distribution. To reduce variance in the final metrics, we repeated training and evaluation 10 times independently and reported the average evaluation metrics on the test sets.

For Deep Ensembles, we utilized MLP and WMLP blocks. Their structure consisted of an input layer that mapped the number of dataset features to a hidden dimension (*hidden_dim*), followed by two hidden layers of size $\textit{hidden_dim} \times \textit{hidden_dim}$, and an output layer of size $\textit{hidden_dim} \times \textit{out_features}$, where *out_features* was set to 1 for regression and to the number of classes for classification. Experiments for Deep Ensembles were conducted for *hidden_dim* values of 64, 128, and 256.

Loss functions were selected based on the task: `MSELoss` for regression and `CrossEntropyLoss` for classification, with `RMSE` and `accuracy` serving as the evaluation metrics, respectively. Optimization was carried out using the `AdamW` optimizer with a learning rate of 1×10^{-3} and a weight decay of 3×10^{-2} . Each network was trained for up to 1000 epochs, with *batch_size* = 256 and early stopping triggered if the validation loss did not improve for 16 consecutive epochs. Training was performed in parallel on 64 CPUs. After each training iteration, we logged the training time, the number of epochs executed, and the performance metric for each of the 64 MLP and WMLP models. Finally, the individual models were aggregated into Deep Ensembles of 2, 4, 8, 16, 32, and 64 networks. For regression tasks, ensemble predictions were computed as the mean of the individual outputs, while for classification tasks the logits were averaged and the final prediction was determined via the `argmax` function. For each ensemble, both the ensemble performance metric and an interpolation metric—derived from averaging the model weights—were recorded.

5.1.2 MOE AND MOIE

In experiments with MoE and MoIE, we used both MLP and WMLP architectures, along with the same loss functions, evaluation metrics, training procedures, and optimizer parameters as described in Section 5.1.1. For these experiments, the expert hidden dimension was fixed at 64. In the WMLP architecture, the number of fixed weights per output unit, n_{fix} , was set to 2 for the input layer and 3 for subsequent layers. The number of experts was varied among [2, 4, 8, 16, 32, 64]. We conducted experiments for all models described in Sections 4.2 and 4.3.

5.2 RESULTS

Figure 1 presents the experimental results, showing the average performance improvements in test metrics across different random seeds. Specifically, we report accuracy for classification tasks and RMSE for regression tasks, measuring improvement relative to the average performance of a single neural network. The results are presented for each dataset and hidden dimension configuration and indicate that Deep Ensembles with WMLP models improve significantly more than with MLP models and this improvement increases as the ensemble size increases.

A possible explanation for this behavior could be that WMLP deep ensembles perform worse than MLP ensembles in terms of absolute test metric values. However, this is not the case, as demonstrated in Appendix A.2. Given that WMLP models retain the universal approximation property, as shown in Lim et al. (2024), we believe this is a promising finding that could encourage the adoption of asymmetric neural networks in ensembles for practical applications.

Likewise, Figure 2 shows the relative performance of MoE and MoIE with a varying number of experts compared to their corresponding models with two experts. As discussed in Section 5.1.2, the hidden size of each expert remains constant. Although MoE with WMLP experts and MoIE with WMLP experts tend to outperform their counterparts with MLP experts on 4 out of 5 datasets, the improvements are less convincing compared to Deep Ensembles. We also report absolute metrics in Appendix A.2.

One potential reason for unclear results in MoE and MoIE might be that the models tend to overfit, meaning that as the number of parameters increases, test metrics deteriorate. We did not apply any regularization techniques to the neural network architectures to avoid overcomplicating the analysis. However, addressing this issue is essential, and the experimental setup for MoE and MoIE should be adjusted in future work.

6 CONCLUSION

In this paper, we empirically demonstrated that the performance of Deep Ensembles improves significantly with increasing ensemble size when using W-Asymmetric MLP models compared to vanilla MLP models. This result may serve as a first step toward understanding the practical impact of reducing symmetry in neural networks.

However, based on our experiments, we cannot conclude that W-Asymmetric MLP improves the performance of either the Mixture of Experts (MoE) or the Mixture of Interpolated Experts (MoIE) models. As discussed in Section 5.2, the experimental setup for MoE should be refined in future work.

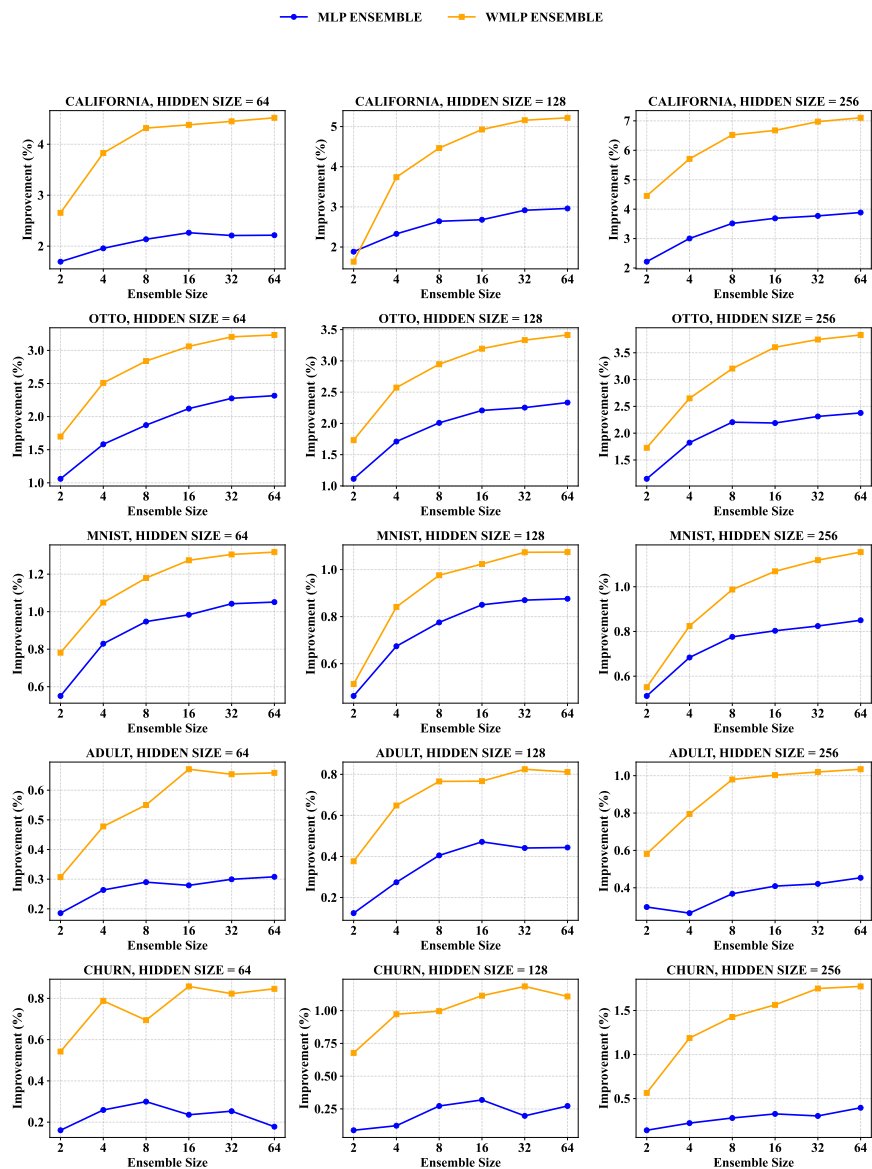


Figure 1: Deep ensembles’ relative improvement in performance. The graphics depicts the relative improvement in performance of both MLP and WMLP models compared to a single MLP and WMLP neural network, respectively.

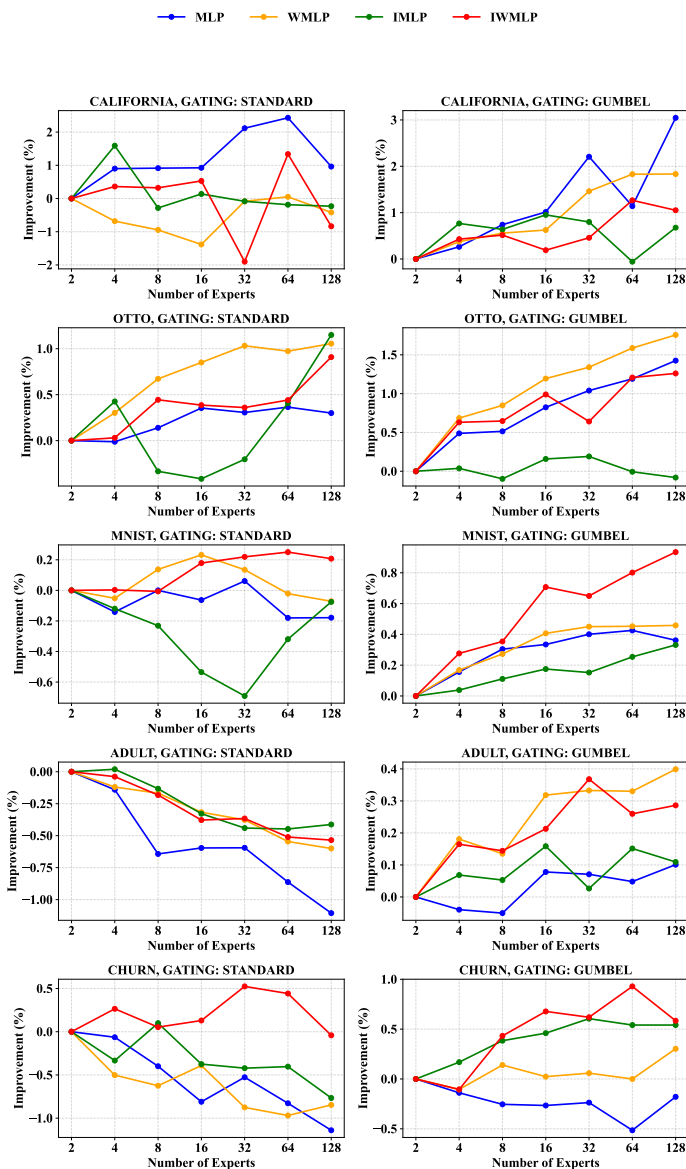


Figure 2: MoE and MoIE relative improvement. In these graphics, MLP represents MoE with vanilla MLP experts, WMLP denotes MoE with WMLP experts, IMLP corresponds to MoIE with vanilla MLP experts, and IWMLP refers to MoIE with WMLP experts. The relative improvement of all models is shown in comparison to their corresponding model architectures with two experts.

REFERENCES

- Vijay Badrinarayanan, Bamdev Mishra, and Roberto Cipolla. Understanding symmetries in deep networks. *arXiv preprint arXiv:1511.01029*, 2015.
- Andrei Chernov. Moe vs. mlp on tabular data. *arXiv preprint arXiv:2502.03608*, 2025.
- Li Deng. The mnist database of handwritten digit images for machine learning research [best of the web]. *IEEE signal processing magazine*, 29(6):141–142, 2012.
- Nan Du, Yanping Huang, Andrew M Dai, Simon Tong, Dmitry Lepikhin, Yuanzhong Xu, Maxim Krikun, Yanqi Zhou, Adams Wei Yu, Orhan Firat, et al. Glam: Efficient scaling of language models with mixture-of-experts. In *International Conference on Machine Learning*, pp. 5547–5569. PMLR, 2022.
- William Fedus, Jeff Dean, and Barret Zoph. A review of sparse expert models in deep learning. *arXiv preprint arXiv:2209.01667*, 2022.
- Charles Godfrey, Davis Brown, Tegan Emerson, and Henry Kvinge. On the symmetries of deep learning models and their internal representations. *Advances in Neural Information Processing Systems*, 35:11893–11905, 2022.
- Dan Hendrycks and Kevin Gimpel. Gaussian error linear units (gelus). *arXiv preprint arXiv:1606.08415*, 2016.
- Ron Kohavi et al. Scaling up the accuracy of naive-bayes classifiers: A decision-tree hybrid. In *Kdd*, volume 96, pp. 202–207, 1996.
- Richard Kurle, Ralf Herbrich, Tim Januschowski, Yuyang Bernie Wang, and Jan Gasthaus. On the detrimental effect of invariances in the likelihood for variational inference. *Advances in Neural Information Processing Systems*, 35:4531–4542, 2022.
- Balaji Lakshminarayanan, Alexander Pritzel, and Charles Blundell. Simple and scalable predictive uncertainty estimation using deep ensembles. *Advances in neural information processing systems*, 30, 2017.
- Derek Lim, Theo Moe Putterman, Robin Walters, Haggai Maron, and Stefanie Jegelka. The empirical impact of neural parameter symmetries, or lack thereof. *arXiv preprint arXiv:2405.20231*, 2024.
- Vinod Nair and Geoffrey E Hinton. Rectified linear units improve restricted boltzmann machines. In *Proceedings of the 27th international conference on machine learning (ICML-10)*, pp. 807–814, 2010.
- Behnam Neyshabur, Russ R Salakhutdinov, and Nati Srebro. Path-sgd: Path-normalized optimization in deep neural networks. *Advances in neural information processing systems*, 28, 2015.
- R Kelley Pace and Ronald Barry. Sparse spatial autoregressions. *Statistics & Probability Letters*, 33(3): 291–297, 1997.
- Fabrizio Pittorino, Antonio Ferraro, Gabriele Perugini, Christoph Feinauer, Carlo Baldassi, and Riccardo Zecchina. Deep networks on toroids: removing symmetries reveals the structure of flat regions in the landscape geometry. In *International Conference on Machine Learning*, pp. 17759–17781. PMLR, 2022.
- Arya A Pourzanjani, Richard M Jiang, and Linda R Petzold. Improving the identifiability of neural networks for bayesian inference. In *NIPS workshop on bayesian deep learning*, volume 4, pp. 31, 2017.
- Joan Puigcerver, Carlos Riquelme, Basil Mustafa, and Neil Houlsby. From sparse to soft mixtures of experts. *arXiv preprint arXiv:2308.00951*, 2023.

Carlos Riquelme, Joan Puigcerver, Basil Mustafa, Maxim Neumann, Rodolphe Jenatton, André Susano Pinto, Daniel Keysers, and Neil Houlsby. Scaling vision with sparse mixture of experts. *Advances in Neural Information Processing Systems*, 34:8583–8595, 2021.

Jonas Gregor Wiese, Lisa Wimmer, Theodore Papamarkou, Bernd Bischl, Stephan Günnemann, and David Rügamer. Towards efficient mcmc sampling in bayesian neural networks by exploiting symmetry. In *Joint European Conference on Machine Learning and Knowledge Discovery in Databases*, pp. 459–474. Springer, 2023.

Seniha Esen Yuksel, Joseph N Wilson, and Paul D Gader. Twenty years of mixture of experts. *IEEE transactions on neural networks and learning systems*, 23(8):1177–1193, 2012.

A APPENDIX

A.1 SUMMARY OF DATASETS

Table 1 provides a summary of the datasets used in this paper.

Table 1: Datasets description

Dataset	Task	Instances	Feature Details	Target Variable
Churn Modelling	Binary Classification	10,000	Customer attributes (e.g., CreditScore, flagGeography, Gender, Age, Tenure, Balance, NumOfProducts)	Customer churn (Exited: yes/no)
Otto Group Product	Multi-class Classification	61,878	93 anonymized numerical features (feat_1 to feat_93)	Product category (9 classes)
Adult Income	Binary Classification	48,842	Mixed continuous and categorical variables (e.g., age, workclass, education, occupation, etc.)	Income level (“>50K” as 1, “<=50K” as 0)
California Housing Prices	Regression	20,640	8 numerical predictors (MedInc, HouseAge, AveRooms, AveBedrms, Population, AveOccup, Latitude, Longitude)	Median house value (in \$100K units)
MNIST	Multi-class Classification	70,000	Preprocessed rectified into a single vector 28×28 pixel grayscale images (784 features per image)	Handwritten digit (10 classes: 0–9)

A.2 ABSOLUTE METRICS FOR ALL MODELS ON TEST DATASET

Figures 3 and 4 present the absolute results of the experiments described in Section 5. In Figure 3, the change of the relevant metric for deep ensembles using both MLP and WMLP models is shown as a function

of ensemble size. The bold lines indicate the mean performance across different random seeds, while the shaded regions represent the \pm one standard deviation intervals. Additionally, the figure displays the mean metric values and intervals for a baseline, which were calculated by aggregating the test metrics of 64 single MLP and 64 single WMLP models; these baseline values were subsequently used in Figure 1. It can be observed that the metric improves as the ensemble size increases. Notably, although WMLP models may yield inferior performance when used individually, the WMLP ensemble tends to outperform the MLP ensemble.

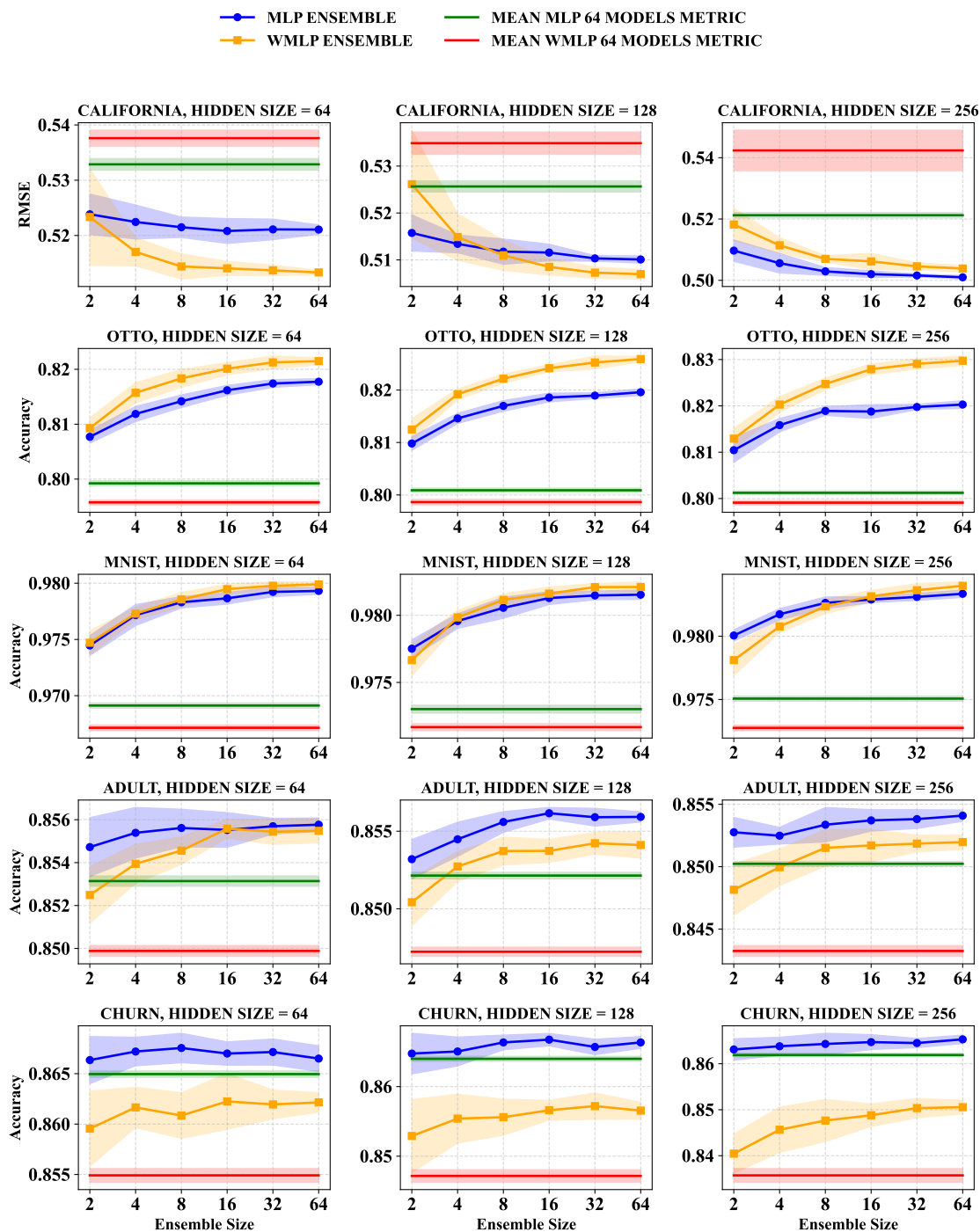


Figure 3: Deep ensemble absolute metrics.

Similarly, Figure 4 illustrates the change of the corresponding metric for MoE and MoIE models as a function of the number of experts. Analogous to Figure 3, the plot shows the mean performance along with the \pm standard deviation intervals obtained from aggregating results over various random seeds. The baseline values corresponding to the case of two experts were used to compute the relative improvements shown in Figure 2. It is evident that the use of Gumbel-softmax leads to better performance compared to the standard softmax, and, in most cases, MoE with WMLP experts or MoIE with WMLP (IWMLP) achieves higher quality than MoE with MLP experts or MoIE with MLP/WMLP, respectively.

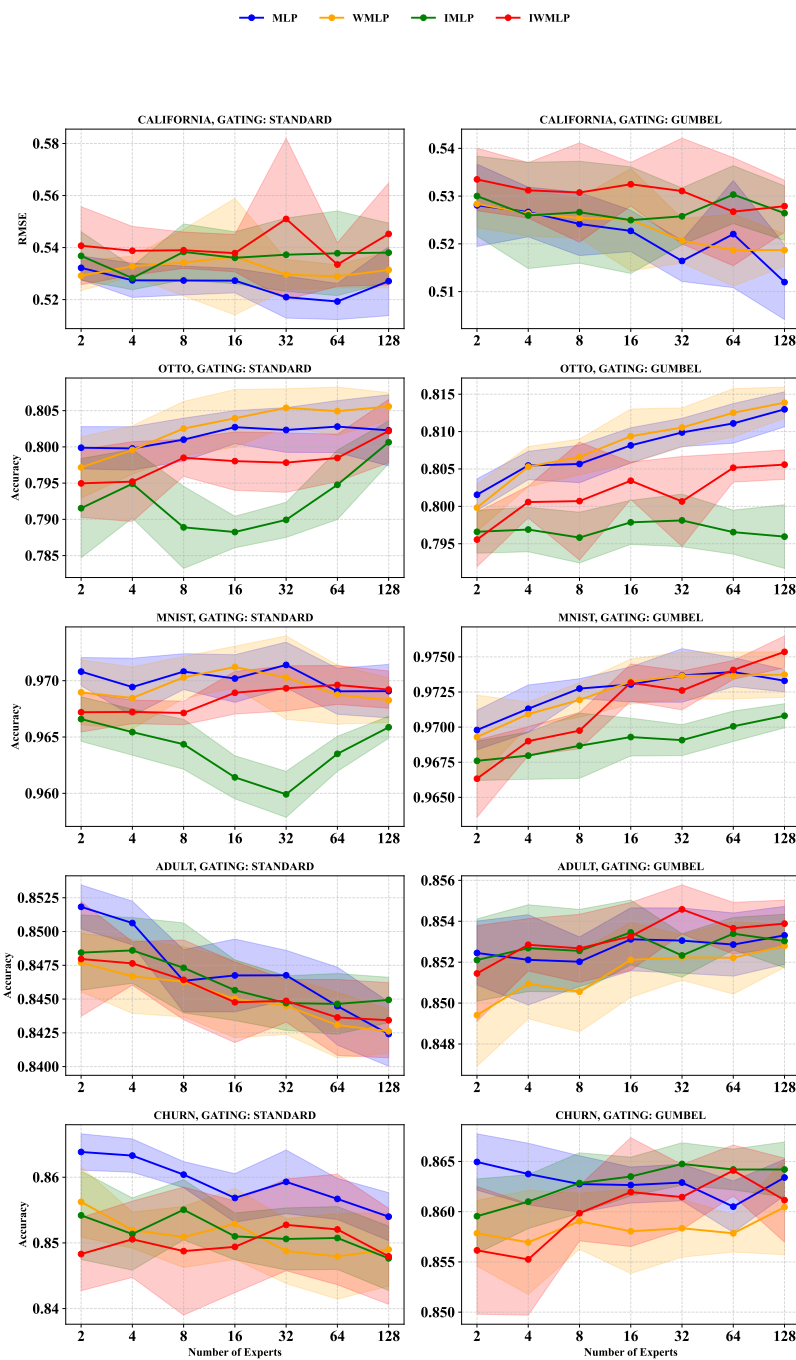


Figure 4: MoE/MoIE absolute metrics.